Photoexcitations in polyacetylene

L. Lauchlan,* S. Etemad,† T.-C. Chung,‡ A. J. Heeger,† and A. G. MacDiarmid‡
Laboratory for Research on the Structure of Matter, University of Pennsylvania, Philadelphia, Pennsylvania 19104
(Received 27 April 1981; revised manuscript received 29 June 1981)

The results of experimental studies of photoluminescence and photoconductivity in *cis*- and *trans*-$(CH)_x$ are presented. For *cis*-$(CH)_x$, we find recombination luminescence in the scattered light spectrum at 1.9 eV, near the interband absorption edge. The luminescence turns on sharply for excitation energies greater than 2.05 eV, implying a Stokes shift of 0.15 eV. Studies of the temperature dependence ($T \geq 7$ K) show no loss of luminescence intensity even at temperatures as high as 300 K. Isomerization of the same sample quenches the luminescence; we find no indication of luminescence near the interband absorption edge of *trans*-$(CH)_x$ even at temperatures as low as 7 K. These results are discussed in the context of parallel phototransport studies. The quenching of the luminenscence upon *cis-trans* isomerization is concurrent with the appearance of a large photoconductive response. The photoconductivity in *trans*-$(CH)_x$ has a threshold at 1.0 eV, well below the interband absorption edge at 1.5 eV, implying the presence of states deep inside the gap. The observation of luminescence in *cis*-$(CH)_x$, but not in *trans*-$(CH)_x$, and the observation of photoconductivity in *trans*-$(CH)_x$, but not in *cis*-$(CH)_x$ provide confirmation of the proposal that solitons are the photogenerated carriers. In *trans*-$(CH)_x$, the degenerate ground state leads to free soliton excitations, absence of band-edge luminescence, and photoconductivity. In *cis*-$(CH)_x$ the nondegenerate ground state leads to confinement of the photogenerated carriers, absence of photoconductivity, and to the observed recombination luminescence.

I. INTRODUCTION

The linear chain polymer, polyacetylene, $(CH)_x$, is of general interest since the structure of the *trans*-$(CH)_x$ polymer chain exhibits a broken symmetry and has a twofold degenerate ground state. As a result, one expects solitonlike excitations, in the form of bond-alternation domain walls, connecting the two degenerate phases. The properties of solitons in $(CH)_x$ have been explored theoretically in several recent papers, which show that the coupling of these conformational excitations to the π electrons leads to unusual electrical and magnetic properties.[1–4] The possibility of experimental studies of such solitons in polyacetylene, therefore, represents a unique opportunity to explore nonlinear phenomena in condensed-matter physics.

Previous studies have focused on the magnetic properties of the neutral soliton defects in undoped *trans*-$(CH)_x$ and on the question of whether the doping proceeds via the soliton mechanism.[1] The high mobility of the magnetic defects together with the remarkable anisotropy in the spin diffusion constant have demonstrated that the neutral magnetic species which appear in *trans*-$(CH)_x$ upon isomerization are bond-alternation domain walls, or neutral solitons.[5–7] Moreover, analysis of the experimentally determined infrared,[8–10] optical,[11] and magnetic properties[12–14] of *trans*-$(CH)_x$ at dilute doping levels have provided detailed evidence of the generation of charged solitons through doping, and of the important role of charged solitons in determining the physics and chemistry of polyacetylene.

Interest in photoexcitation studies of $(CH)_x$ has been stimulatd by the recent calculations of Su and Schrieffer,[15] who considered direct injection of an *e-h* pair and studied the time evolution of the system. Their principal result was the conclusion that in *trans*-$(CH)_x$ a photoinjected *e-h* pair evolves to a soliton-antisoliton pair in a time of order the reciprocal of an optical-phonon frequency. This is the central experimental question addressed in the present paper: Are solitons photogenerated in polyacetylene?

The proposed photogeneration of charged solitons has clear implications which can be checked through studies of photoluminescence and photoconductivity.[16,17] We therefore present and discuss in this paper the experimental results obtained with these two complementary techniques in *cis*- and *trans*-$(CH)_x$. In the scattered light spectrum from *cis*-$(CH)_x$, we find a relatively broad luminescence structure peaking at 1.9 eV, near the interband absorption edge, together with a series of multiple-order Raman lines. Through measurements of the excitation spectrum,

we have found that the luminescence turns on sharply for excitation energies greater than 2.05 eV, implying a Stokes shift of 0.15 eV. The main peak in the luminescence structure at 1.9 eV has a half-width of about 0.1 eV and a Lorentzian energy profile. The luminescence intensity is essentially independent of temperature from 7 K to room temperature. Isomerization of the same sample to *trans*-$(CH)_x$ quenches the luminescence; we find no indication of luminescence near the interband absorption edge of *trans*-$(CH)_x$ even at temperatures as low as 7 K. These luminescence data are discussed in the context of parallel phototransport studies. We find that the quenching of the luminescence upon *cis-trans* isomerization is concurrent with the appearance of a large photoconductive response. The photoconductivity in *trans*-$(CH)_x$ has a threshold at 1.0 eV, well below the interband absorption edge at 1.5 eV, implying the presence of states deep inside the gap.

The observation of luminescence in *cis*-$(CH)_x$ but not in *trans*-$(CH)_x$, and the observation of photoconductivity in *trans*-$(CH)_x$ but not in *cis*-$(CH)_x$ provide confirmation of the proposal that solitons are the photogenerated carriers. In *trans*-$(CH)_x$, the degenerate ground state leads to free-soliton excitations, absence of the band-edge luminescence and photoconductivity. In *cis*-$(CH)_x$ the nondegenerate ground state leads to confinement of the photogenerated carriers, absence of photoconductivity, and to the observed recombination luminescence.

II. EXPERIMENTAL RESULTS

A. Photoluminescence of *cis*- and *trans*-$(CH)_x$

For Raman and photoluminesence studies, thin (2–5 μm) films of polyacetylene were polymerized[18] at −78 ° C directly onto flat aluminum substrates. These films were used in order to minimize laser heating and to prevent thermal isomerization of *cis*-$(CH)_x$ during the course of the measurements. The temperature difference across a $(CH)_x$ film of thickness ~5 μm is estimated to be less than one degree for a typical light flux of 100 mW/cm^2. In order to thermally anchor the polyacetylene films, the Al substrates were heat sunk with "Cry-Con" conductive grease to the cold tip of an Air Products Helitran liquid flow refrigerator. Using this configuration, substrate temperatures could be controlled from 7 to 300 K.

Optical measurements employed a standard 90° scattering configuration. Raman and photoluminescence spectra were taken using a Spex 1401 double monochromator equipped with photon-counting detection. In this study, excitation lines (4579 to 6471 Å) from either an argon-ion or a krypton-ion laser were used. In addition, a Rhodamine-6G dye laser was used for obtaining the excitation spectrum of the photoluminescence peak in *cis*-$(CH)_x$.

In Fig. 1, we show the photoluminescence and the multiple overtone Raman structure from *cis*-$(CH)_x$ obtained at 7 K using 4880-Å (2.54-eV) laser line excitation. The fact that the emission is always centered at 1.9 eV, independent of excitation frequency, demonstrates that it is intrinsic photoluminescence of *cis*-$(CH)_x$. The luminescence peak is replotted in Fig. 2 and compared with the energy dependence of the absorption coefficient[19] for *cis*-$(CH)_x$, $\alpha_c(\omega)$. The peak energy is just below the steep increase in the absorption coefficient. We find that over the full temperature range studied (7 to 300 K) the luminescence peak occurs at 1.9 eV with no observable shift in frequency.

The excitation spectrum (i.e., the intensity dependence of the photoluminescence as a function of laser excitation frequency) is shown in Fig. 3. Note that although the luminescence is centered at 1.9 eV, excitation frequencies above 2.05 eV are required to excite the luminescence. The energy difference between the excitation threshold (2.05 eV) and the energy of luminescence (1.9 eV) is interpreted as a Stokes shift, presumably arising from the formation of a lattice distortion around the photoexcited *e-h* pair. Above the relatively sharp excitation threshold, the luminescence intensity is essentially independent

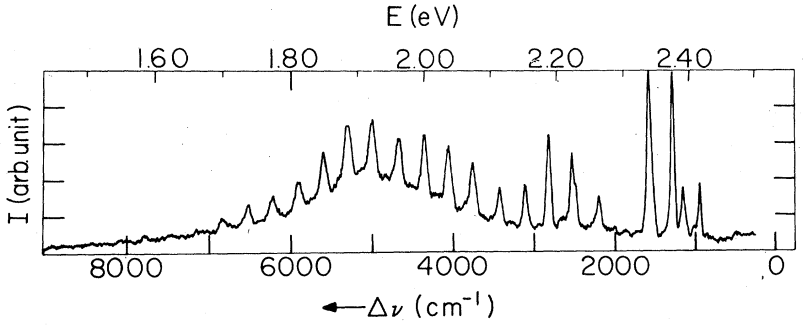

FIG. 1. Photoluminescence and multiple overtone Raman structure from *cis*-$(CH)_x$ obtained at 7 K. The scattered light intensity is plotted as a function of frequency shift ($\Delta\nu$) away from the 2.54-eV laser excitation. The luminescence peaks at 1.9 eV.

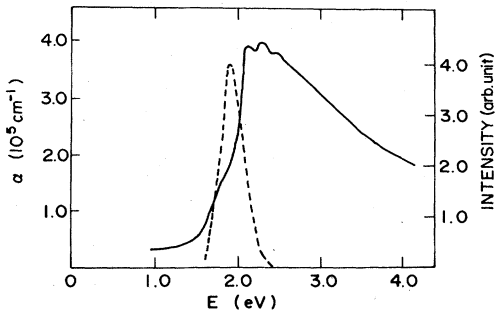

FIG. 2. Comparison of the photoluminescence spectrum (– – –) and the interband absorption spectrum (solid curve) for *cis*-$(CH)_x$.

of excitation frequency up to the maximum energy available. As expected, the multiple Raman lines shift with the laser frequency.

The luminescence spectrum of *cis*-$(CH)_x$ is replotted in Fig. 4, after subtracting the multiple order Raman lines from the results presented in Fig. 1. The solid curve on Fig. 4 is a fit of a Lorentzian line shape to the luminescence peak. The Lorentzian (half-width at half maximum of 0.13 eV) is a good fit on the long-wavelength side, but falls below the experimental curve above ~1.95 eV, suggesting a weak second peak centered near 2.0 eV. The dashed curve shows the effect of adding a second Lorentzian centered at 2.0 eV (half-width ≃0.04 eV) with a peak height of 7.0% of the main line. The long tails ap-

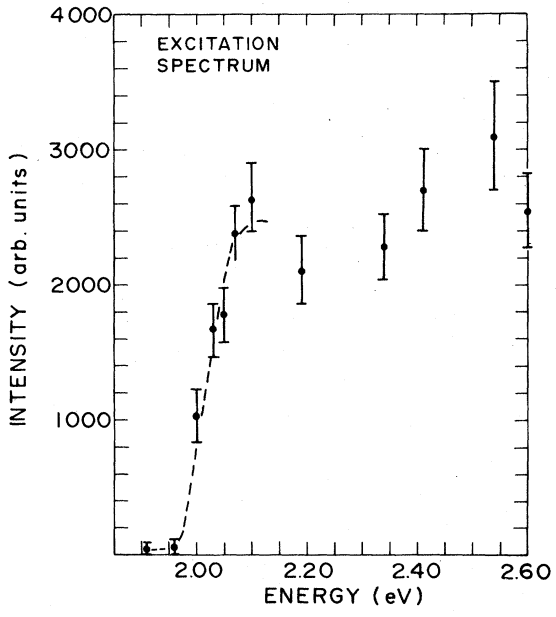

FIG. 3. Excitation spectrum for the luminescence from *cis*-$(CH)_x$. The energy difference between the excitation threshold (2.05 eV) and the energy of luminescence (1.9 eV) is interpreted as a Stokes shift.

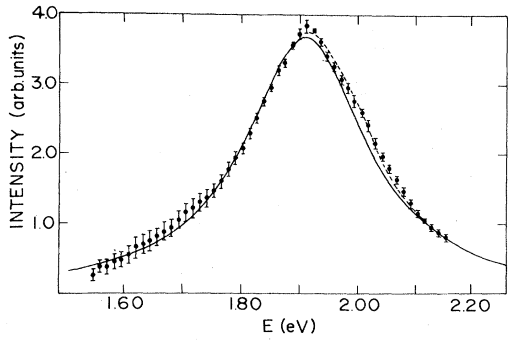

FIG. 4. Replot of the luminescence spectrum of *cis*-$(CH)_x$ after subtracting the multiple-order Raman lines. The solid curve is a fit of a Lorentzian (half-width at half maximum of 0.13 eV). The shoulder on the high-energy side suggests a weak second peak at 2.05 eV; the dashed curve shows the effect of adding a second Lorentzian to the fit (see text).

pear inconsistent with a Gaussian shape, and attempts to fit to a Gaussian line shape were unsuccessful. The width of the main luminescence peak is essentially independent of temperature as shown on Fig. 5. A third weak luminescence appears to exist near 2.2 eV (near $\Delta\nu \simeq 2700$ cm^{-1} on Fig. 1). Due to the presence of the strong multiple order Raman lines, there is an uncertainty of about ±0.05 eV in the estimated positions of the two weak secondary maxima.

The measured luminescence intensity shows relatively little temperature dependence, up to 150 K. At higher temperature, a decrease results from partial isomerization of the initially *cis*-$(CH)_x$ film. We have monitored the relative *cis-trans* content with the principal Raman lines[20] and normalized the luminescence

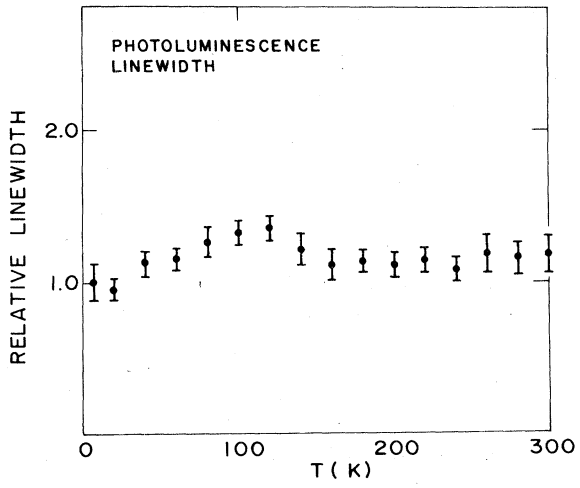

FIG. 5. Temperature dependence of the photoluminescence linewidth; the full width at half maximum is approximately 0.25 eV.

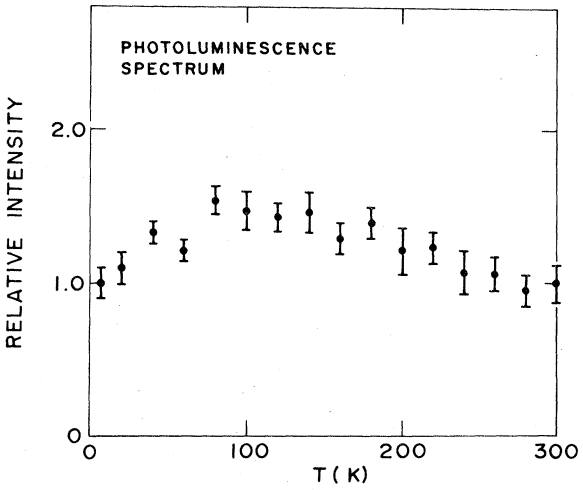

FIG. 6. Temperature dependence of the luminescence intensity from *cis*-$(CH)_x$. The results were corrected for *in situ* isomerization during the course of the measurements by monitoring the principal *cis* and *trans* Raman lines (see text).

intensity to the fractional *cis*-$(CH)_x$ content in the film. The resulting temperature dependence of the luminescence intensity of *cis*-$(CH)_x$ is shown on Fig. 6. The results show no significant decrease in intensity even at temperatures as high as 300 K.

In the course of their extensive studies of Raman scattering from polyacetylene, Lichtmann *et al.*[21] also observed the 1.9-eV luminescence from *cis*-$(CD)_x$ and *cis*-$(CH)_x$ at 77 K. Their results are equivalent to ours at 77 K. The results plotted in Figs. 1 through 6 provide the first measurements of the excitation spectrum, The Stokes shift, and the temperature dependence of the intensity and width of the photoluminescence peak.

After completing the measurements on *cis*-$(CH)_x$ the same film was isomerized by heating in vacuum at approximately 160 °C for about 10 min. Thermal isomerization to *trans*-$(CH)_x$ quenches the luminescence peak as shown in Fig. 7. There is no photoluminescence from *trans*-$(CH)_x$ in the vicinity of the steep rise in interband absorption; i.e., near 1.6 eV. The intensity of any luminescence peak from *trans*-$(CH)_x$ in the range of our measurements (1.4 to 2.5 eV) is less than that of the *cis*-$(CH)_x$ peak at 1.9 eV by at least a factor of 50.

B. Photoconductivity (Ref. 16) of *cis*- and *trans*-$(CH)_x$

The photoconductivity studies were carried out at room temperature on thin film samples (thickness of a few micrometers) polymerized directly on glass substrates. Experiments utilized primarily the surface cell configuration using Ohmic contacts; similar results were obtained using sandwich cells. Note that the flat excitation spectrum for photoluminescence in combination with a frequency-dependent absorption coefficient with magnitude greater than 10^5 implies that surface recombination is not of major importance.[22] Measurements were carried out in the range 0.6–3.0 eV using phase-sensitive detection (13 Hz) of the voltage change across a resistor in series with the sample. Where necessary, corrections were made for transmitted light. The light to dark current ratio depended on sample treatment, doping and/or compensation, and varied from 10^{-6} to 10^{-1} at 2.0 eV with 10^{14} photons/cm^2 sec.

In Fig. 8 the logarithm of the photocurrent (I_{ph}), normalized to the number of absorbed photons, is shown as a function of photon energy. Results obtained from different sample preparations show a large variation in the magnitude of the photoresponse below 1 eV. The inset in Fig. 8 shows a comparison of the same data (curve A) with results from three other samples of varying quality in order to point out the sample dependence of the photocurrent spectrum. A distinct common feature, however, is the exponential rise above 1 eV seen clearly in Fig. 8. Our experience is that those films which showed significant response below 1 eV were of poorer quality as

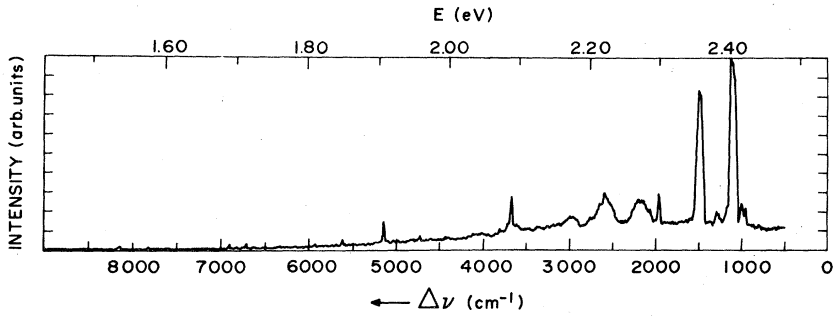

FIG. 7. Scattered light spectrum from *trans*-$(CH)_x$ obtained at 7 K using 2.54-eV laser excitation. The intensity of any luminescence near the onset of interband absorption (1.5–1.6 eV) is less than that of the *cis*-$(CH)_x$ peak (Fig. 1) by at least a factor of 50. The broad background is the luminescence from the Al substrate due to the presence of pinholes in the thin $(CH)_x$ film.

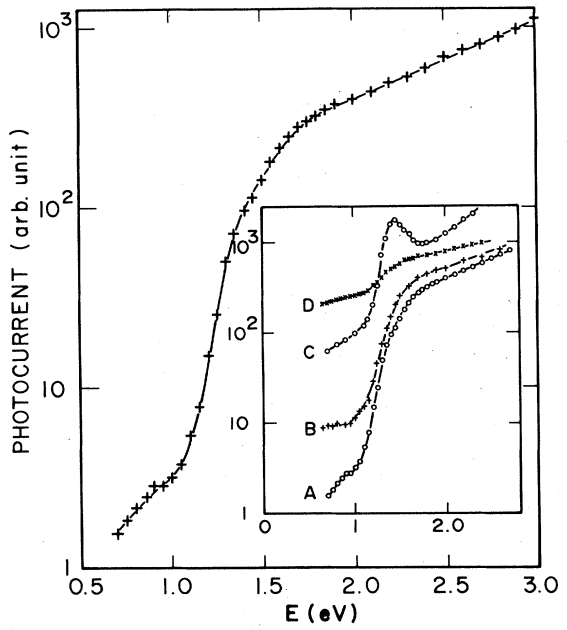

FIG. 8. Photocurrent vs photon energy for *trans*-$(CH)_x$. The inset shows a comparison of the same data (curve A) with results from three other samples of varying quality. Generally, films which showed significant response below 1 eV were of poorer quality as characterized by visual appearance. Compensation with ammonia decreased the low energy response converting the I_{ph} spectrum from curve D to curve A.

characterized by visual appearance. Moreover, compensation with ammonia decreased the low-energy response converting the I_{ph} spectrum from curve D to curve A. Earlier results[23] on compacted powders showed an increase in I_{ph} by only a factor of 4 near 1 eV compared with the two orders of magnitude increase indicated in Fig. 8.

Measurements of I_{ph} in *cis*-$(CH)_x$ were also attempted. Under similar conditions any photoresponse in samples of 80% *cis*-rich $(CH)_x$ was below the noise level of our experiment. The upper limit on I_{ph} in *cis*-$(CH)_x$ is more than three orders of magnitude smaller than I_{ph} in *trans*-$(CH)_x$. *In situ* isomerization of the same film resulted in the sizable I_{ph} shown in Fig. 8.

The photocurrent spectrum for *trans*-$(CH)_x$ is replotted in Fig. 9 and compared with the energy dependence of the absorption coefficient for *trans*-$(CH)_x$, $\alpha_t(\omega)$.[19] In contrast to earlier suggestions,[24] we note that the photoconductivity sets on well below the interband absorption, suggesting the presence of states deep inside the gap. This is clearly shown in the inset to Fig. 9 where the photoresponse and absorption are compared on a linear scale. The threshold for the generation of free carriers is better seen in the logarithmic plot of I_{ph} versus photon energy (Fig. 9). The absence of structure in $\alpha_t(\omega)$ at the onset of

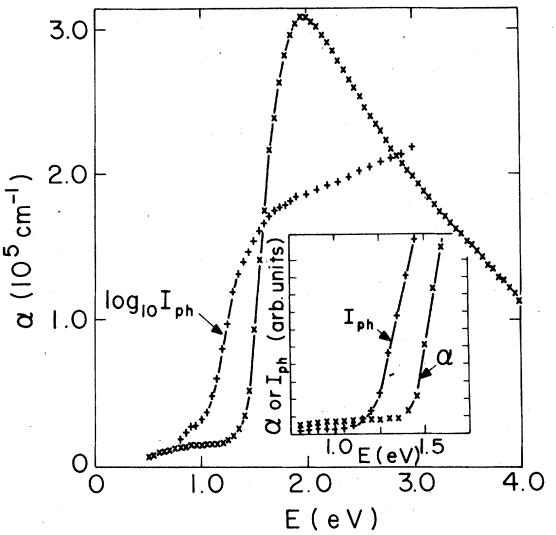

FIG. 9. Comparison of the photocurrent ($\log_{10} I_{ph}$) and optical absorption coefficient (α) as a function of photon energy. Note the threshold of I_{ph} near 1 eV, well below the onset of interband absorption. I_{ph} and α are compared on a linear scale in the inset.

I_{ph} implies a low quantum efficiency at threshold. The free carrier generation efficiency rises exponentially above the threshold and changes to a slow increase above the onset of the interband transition.

The photoconductivity results do not result from bolometric effects. The observation (Fig. 9) that I_{ph} increases by nearly two orders of magnitude in the frequency interval where α_t has negligible energy dependence rules out heating effects on the I_{ph} threshold. Furthermore, the observation that the light-to-dark current ratio can be varied by more than five orders of magnitude by doping and/or compensation clearly demonstrates that I_{ph} does not scale with the dark conductivity as would be expected from absorption-induced heating (at constant voltage). For example after compensation with ammonia, the photoconductivity of *trans*-$(CH)_x$ was readily detected even though the dark conductivity decreased by four orders of magnitude. At this point, the dark resistance was comparable to that of the *cis*-$(CH)_x$ sample where no signal was observed. Finally, we note that the energy dependence of the photocurrent (Fig. 9) closely resembles the photovoltaic quantum efficiency obtained from junction studies[25,26] with *trans*-$(CH)_x$. Thus, the photoresponse shown in Fig. 9 is genuine photoconductivity resulting from photogenerated carriers in *trans*-$(CH)_x$.

In the course of these studies, photoluminescence and Raman studies were carried out on about five samples, and photoconductivity studies were done on more than 20 samples. The luminescence results showed excellent reproducibility. The absolute magnitude of the photoconductivity and the relative size

of the photoresponse below 1.0 eV varied from sample to sample; however, the principal spectral features and overall shape of the response curve were quite reproducible.

III. DISCUSSION OF THE EXPERIMENTAL RESULTS

The identification of the photogenerated carriers is of fundamental importance: Are they electron-hole pairs or soliton-antisoliton pairs? As indicated above, Su and Schrieffer[15] have shown that in the presence of the *e-h* pair the lattice is unstable and (in a time of the order of the reciprocal of an optical-phonon frequency) distorts to form a soliton-antisoliton pair. Thus, whatever the initial process, soliton formation is expected to occur in *trans*-$(CH)_x$ in a time of order of 10^{-13} sec.

In traditional semiconductors, photoconductivity and recombination luminescence are intimately related, and both are observed after photoexcitation. Photoconductivity indicates the presence of free carriers generated by the absorbed photons. Although the subsequent recombination of these photogenerated carriers can take place either radiatively or nonradiatively, recombination luminescence is commonly observed, at least at low temperatures. The fundamental differences between such traditional data and those obtained from polyacetylene can be seen by comparison of the $(CH)_x$ results with results obtained from cadmium sulfide (CdS). The luminescence and multiple order Raman scattering data[27] from CdS are similar to the results obtained from *cis*-$(CH)_x$. However, in CdS, a strong photoconductive response is observed for photon energies just above the band edge,[28] whereas in *cis*-$(CH)_x$ significant photogeneration of free carriers is not observed even for photon energies 1 eV above the band edge. Isomerization to *trans*-$(CH)_x$ quenches the luminescence at all temperatures, but turns on the photoconductivity. In neither isomer is the traditional combination of effects observed. These unique experimental results, therefore, lead us to consider the proposed photogeneration of solitons in more detail.

A schematic diagram of the photogeneration of a charged soliton-antisoliton pair in *trans*-$(CH)_x$ is shown in Fig. 10. The incident photon (for $\hbar\omega \geq 2\Delta$) generates an *e-h* pair within the rigid lattice [Fig. 10(a)]. The system rapidly evolves to a charged soliton pair [Fig. 10(b)] as shown by Su and Schrieffer.[15] After a time of order 10^{-13} sec, their results imply the presence of two kinks separating degenerate regions. Because of the precise degeneracy of the *A* and *B* phases, the two charged solitons are free to move in an applied electric field and contribute to the photoconductivity.

The topological degeneracy in *trans*-$(CH)_x$ is not present in *cis*-$(CH)_x$, so that soliton photogeneration

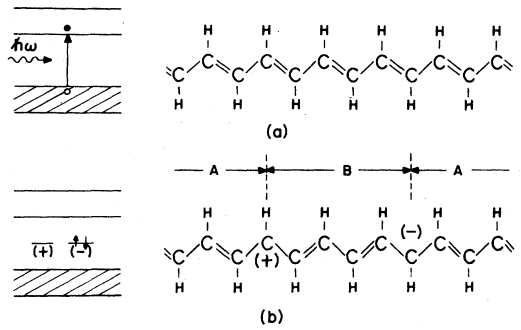

FIG. 10. (a) Band diagram and chemical-structure diagram for *trans*-$(CH)_x$. The band diagram shows schematically the absorption of a photon and the creation of an *e-h* pair. (b) A *trans*-$(CH)_x$ chain containing a charged soliton-antisoliton pair. Since regions *A* and *B* are degenerate, the solitons are free and can move apart with no cost in energy. The corresponding band diagram shows the midgap states associated with the two solitons; one empty (+) and the other doubly occupied (−). The soliton deformations are shown as localized on a single site, whereas the deformation should be spread over about 15 lattice constants.

would not lead to photoconductivity in the *cis* isomer. Since the *cis-transoid* configuration [Fig. 11(a)] has a lower energy than the *trans-cisoid* configuration [Fig. 11(b)], domain walls would separate nondegenerate regions [Fig. 11(c)]. Although neither of the limiting forms of Figs. 11(a) and 11(b) is literally correct, we

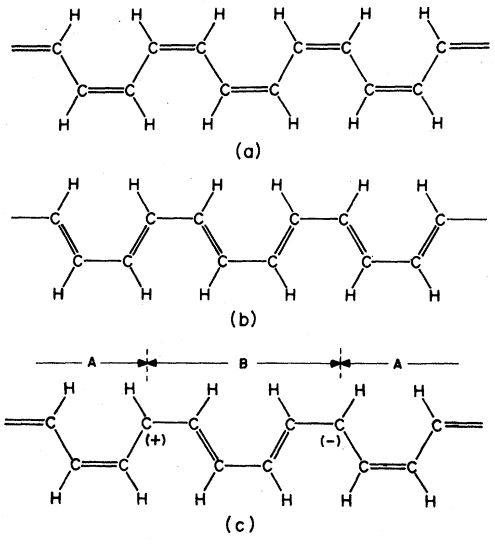

FIG. 11. (a) *cis*-$(CH)_x$; *cis-transoid* configuration (lower energy). (b) *cis*-$(CH)_x$; *trans-cisoid* configuration (higher energy). (c) A *cis*-$(CH)_x$ chain containing a charged soliton-antisoliton pair. Since the regions *A* and *B* are not degenerate, the solitons are *confined;* the farther apart the greater the energy. The soliton deformations are shown as localized on a single site, whereas the deformation should be spread over many lattice sites.

may think of the ground state as essentially equivalent to Fig. 11(a), with the structure of Fig. 11(b) being slightly higher in energy. Consider then the photoexcitation of a charged soliton-antisoliton pair as shown schematically in Fig. 11(c). The energy required is

$$E_{\text{tot}} = 2E_s + n\Delta E_0 \ , \tag{1}$$

where E_s is the energy for creation of a single soliton [analogous to the soliton creation energy in *trans*-$(CH)_x$], n is the number of CH monomers separating the two kinks, and ΔE_0 is the energy difference between the two configurations [Figs. 11(a) and 11(b)], estimated to be a small fraction of the full gap, $2\Delta \simeq 2.0$ eV, in *cis*-$(CH)_x$. Thus, as they begin to form, the two solitons would be "confined," or bound into a polaronlike entity, the farther apart, the greater the energy.[16,17,29] As a result, one expects the photogenerated pair to quickly recombine.

The photoluminescence results thus provide the first confirmation of the soliton photogeneration ideas. The absence of band-edge luminescence in *trans*-$(CH)_x$ even at the lowest temperatures is consistent with the proposed photogeneration of charged soliton-antisoliton pairs. *In this case, band edge luminescence cannot occur since there are no electrons and holes.* The charged soliton pair consists of two kinks with associated midgap states [Fig. 10(b)]. Final recombination of the soliton pair could occur either radiatively (with a large Stokes shift to approximately midgap) or nonradiatively through charge transfer to form two neutral kinks, which subsequently relax to the ground state by multiphonon emission. In either case, there would be no band edge luminescence.

The luminescence results in *cis*-$(CH)_x$ as shown in Figs. 1–6 provide some insight into the dynamics of the system. The energy given off to phonons during the formation of the lattice distortion would lead to a stokes shift of the luminescence relative to the minimum energy needed to make a free *e-h* pair. As indicated above, a Stokes shift of $\Delta E_s = 0.15$ eV is observed relative to the onset of photoexcitation at 2.05 eV. The magnitude of ΔE_s is, however, much less than that expected for the formation of either two free solitons or two free polarons. In the case of two free solitons, the corresponding electronic levels would be near mid-gap with the luminescence energy going to zero in the limit of $(\Delta E_0/2\Delta) \rightarrow 0$. In this limit for a well-separated electron polaron and hole polaron,[17,30] the corresponding luminescence energy would be $\hbar\omega_l = \sqrt{2}\Delta = 1.4\Delta$ with an implied Stokes shift of $\Delta E_s = 0.6\Delta$. The much smaller experimental value of $\Delta E_s \sim 0.07\Delta$, therefore, indicates that the absence of a degenerate ground state in *cis*-$(CH)_x$ has made qualitative changes in the dynamics of photoexcitations in the two isomers.

Brazovskii and Kirova[17] have pointed out that because of the confinement energy [Eq. (1)] the total gap in a commensurate Peierls distorted system arises from a sum of two terms,

$$\tilde{\Delta}(x) = \Delta_l(x) + \Delta_e \ , \tag{2}$$

where $\Delta_l(x)$ is the intrinsic Peierls gap stabilized by π electrons, and Δ_e is the incompressible contribution arising from the σ-electron backbone structure. In *trans*-$(CH)_x$, $\Delta_e = 0$ by symmetry; whereas in *cis*-$(CH)_x$ $\Delta_e \neq 0$ since even in the case of equal bondlengths the transfer integrals alternate. The increase in the optical gap of *cis*-$(CH)_x$ compared with that of *trans*-$(CH)_x$ implies a relatively large Δ_e. Moreover since the presence of Δ_e tends to reduce the divergence leading to the Peierls instability, $\Delta_l^{\text{cis}} < \Delta_l^{\text{trans}}$, so that for *cis*-$(CH)_x$ one expects larger Δ_e than the difference between the optical gaps of the two isomers.

Using this formulation, Brazovskii and Kirova defined the basic confinement parameter $\gamma = \Delta_e/\lambda\Delta$ (where λ is the electron-phonon coupling constant) and developed a detailed theory of the excited states in the presence of confinement. They find for the gap parameter $\Delta(x) = [1 - \delta(x)]$

$$\delta(x) = \tanh\alpha[\tanh(x/\xi^* + \alpha/2) - \tanh(x/\xi^* - \alpha/2)] \ , \tag{3}$$

where α is a variable which depends on Δ_e and Δ_l and is fixed by minimizing the total bipolaron energy, and $\xi^* = \xi_0 \coth\alpha$ with $\xi_0 = \hbar v_F/\Delta \simeq 7a$. For weak confinement the excitation is equivalent to two well-separated domain walls; for strong confinement Eq. (3) describes a shallow bipolaron. On formation of the excitation, two electronic states are pulled inside the gap at $E_p = \pm\Delta/\cosh\alpha$ relative to the gap center. If we *assume* that in *cis*-$(CH)_x$ the optical excitation quickly comes to the minimum energy configuration described by Eq. (3) then the luminescence would occur at $\hbar\omega_l = 2\Delta/\cosh\alpha$, and the Stokes shift would be $\Delta E_s = 2\Delta(1 - 1/\cosh\alpha)$. Using the experimental value, $\Delta E_s = 0.15\Delta$, we obtain $\alpha = 0.4$ and $\gamma \simeq 2.8$ implying relatively strong confinement with $\xi^* \simeq 2.5\xi_0$; i.e., the shallow bipolaron limit. In this context, however, it should be noted that the relatively broad Lorentzian shape of the main emission (see Fig. 4) may result from lifetime broadening. The implied luminescence lifetime would be of the order of the reciprocal or an optical phonon frequency; i.e., comparable to the time scale for soliton (or polaron) formation. If this is indeed the case, the assumption that the optical excitation is in quasiequilibrium at the minimum energy configuration would not be valid. In this case, the small experimental value of ΔE_s would result, at least in part, from recombination *before* the bipolaron distortion is fully

formed. Both time-resolved luminescence and an extension of the theory to include such dynamical effects are required before these results can be understood in greater depth.

The suggestion that confinement of photogenerated carriers plays an important role in *cis*-$(CH)_x$ may provide an explanation for the unusual multiple overtones observed in the Raman spectra.[21] The implied anharmonic "ringing" of the lattice excitations is indicative of strong electron-phonon coupling. Note that whereas the confinement in *cis*-$(CH)_x$ is intrinsic and due to the absence of a degenerate ground state, confinement can be simulated in *trans*-$(CH)_x$ by boundaries. Lichtmann and Fitchen[31] have recently reported band-edge luminescence (near 1.5 eV) and multiple overtones of the *trans*-$(CH)_x$ Raman lines from partially isomerized samples consisting of short segments of *trans*-$(CH)_x$ imbedded in the *cis* isomer. Thus the intense multiple Raman overtones and the band-edge luminescence appear to have a common origin, and they are observed under conditions where the photogenerated carriers are unable to separate. A theoretical analysis of Raman scattering and luminescence for the case of a nearly degenerate ground state is required for further understanding of this rich class of phenomena.

The photoconductivity results provide the second confirmation of soliton photogeneration. The absence of photoconductivity in *cis*-$(CH)_x$ is consistent with the proposed confinement of photogenerated carriers, whereas the observation of photoconductivity in *trans*-$(CH)_x$ indicates the generation of free carriers. The minimum energy required for photogeneration of free positive and negative soliton pairs is $2(2\Delta/\pi) < 2\Delta$.[3,17] Since the direct photogeneration of a soliton pair requires a significant lattice distortion simultaneous with the electronic transition, the quantum efficiency near threshold is expected to be small and to increase exponentially[17] as $\hbar\omega$ approaches 2Δ, in a manner similar to an Urbach tail.[32] For $\hbar\omega \simeq 2\Delta$, the interband transition has a quantum efficiency of order unity for direct *e-h* pair production so that the overall soliton-antisoliton photogeneration process should be only a weak function of energy. The experimental results are in agreement; I_{ph} rises rapidly and exponentially above 1 eV $\simeq 2(2\Delta/\pi)$ and more slowly above 1.5 eV $\simeq 2\Delta$. Thus the spectral dependence of I_{ph} for *trans*-$(CH)_x$ is consistent with photogeneration of charged soliton-antisoliton pairs. The knee in I_{ph} at $\hbar\omega \simeq 2\Delta$, the onset of interband absorption, must be contrasted with the sharp rise typically seen at that point in traditional semiconductors where electrons and/or holes are the photoinjected carriers. In the data of Fig. 9, the major increase in I_{ph} (a factor of 10^2) occurs in the experimental rise *below* the onset of interband absorption. The continued slow increase in both I_{ph} and the junction quantum efficiency above 1.5 eV [with no structure corresponding to $\alpha_t(\omega)$] may indicate the importance of geminate recombination processes.[33]

A broadening of the absorption edge can be expected from static disorder, or from a combination of quantum and thermal fluctuations in $\Delta(x)$, the local energy gap parameter. Such dynamical fluctuations generate random dynamical distortions in the crystal. Since the electronic states that contribute to the absorption edge are determined in accord with the Frank-Condon principle by the instantaneous ($\sim 10^{-16}$ sec) configuration of the lattice, these fluctuations lead to a distribution of short-lived states ($\sim 10^{-13}$ sec) below the band edge. As a result, the absorption edge is smeared and an Urbach tail is generated. For temperatures less than a typical phonon energy ($\hbar\omega_0 \simeq 1500$ cm^{-1}) Brazovskii[17] has shown that the energy dependence of such an Urbach absorption tail varies as

$$\alpha(\omega) \sim \exp\left[-\frac{\Delta}{\hbar\omega_o}\left(2-\frac{\hbar\omega}{\Delta}\right)^{3/2}\right] \tag{4}$$

for $\hbar\omega \leq 2\Delta$. In this case, the associated microfield[16] arises from the quantum fluctuations instead of disorder or optical phonons as is the case for ionic or covalent semiconductors. A fit of the exponential rise of the photocurrent below the band edge (see Fig. 1) to Eq. (4) results in $\hbar\omega_o \simeq 0.2$ eV, in agreement with the lattice dynamic results for *trans*-$(CH)_x$.[10]

The much increased photoconductivity in *trans*-$(CH)_x$ with essentially identical peak absorption in the two isomers implies a major increase in total recombination lifetime upon isomerization. In fact, recent experiments have demonstrated a transient photoconductive decay time in excess of 10^{-3} sec at room temperature.[34] This relatively long decay time is qualitatively consistent with the nonlinearity of the soliton dynamics[35] which would tend to suppress the recombination of soliton-antisoliton pairs. Thus, the absence of band edge luminescence and the appearance of photoconductivity are expected in *trans*-$(CH)_x$ if, in the presence of an *e-h* pair, the lattice is unstable and distorts to form a soliton-antisoliton pair.

Alternative explanations must be carefully considered. The observed band edge luminescence in *cis*-$(CH)_x$ (with a small Stokes shift) may simply result from conventional *e-h* pair recombination. However, our inability to observe photoconductivity in *cis*-$(CH)_x$ strongly suggests that the photogenerated carriers are bound and unable to contribute to the phototransport. Although this could result directly from Coulomb binding of the *e-h* pairs into neutral excitons, the nearly identical peak absorption coefficient and the small increase in the energy gap on going from *trans*- to *cis*-$(CH)_x$ argue against significant differences in the strength of the effective Coulomb

interaction in the two isomers. Moreover, the close quantitative agreement between theory and experiment obtained in the study of the soliton-induced infrared-active vibrational modes provides solid evidence of the basic validity of the one-electron approach with Coulomb interactions playing only a minor role.[9,10] The fact that no photoconductivity is observed in *cis*-$(CH)_x$ even for incident photon energies as high as 3 eV would require an exciton binding energy in excess of 1 eV. Furthermore,the relatively flat excitation spectrum (Fig. 4) above thereshold is not consistent with an exciton bound state near the band edge. Finally, the absence of a significant decrease in luminescence intensity even at temperatures as high as 300 K is not consistent with a simple bound state.

The nonradiative recombination of photoexcited *e-h* pairs in disordered semiconductors is usually found to be an activated process.[22] This arises primarily from the localized nature of the band-edge (or gap) states from which the photoexcited electron must tunnel in order to escape radiative recombination. As a result, in such semiconductors the photoluminescence efficiency increases exponentially upon lowering the temperature. The fact that no luminescence is observed from *trans*-$(CH)_x$ even at $T=7$ K is therefore unusual and of special interest, particularly in the context of the temperature-independent luminescence intensity in *cis*-$(CH)_x$.

The Stokes-shifted luminescence spectrum together with the multiple-order Raman lines indicate the importance of electron-phonon coupling in *cis*-$(CH)_x$. As a result, a lattice deformation is expected to accompany the photoexcited state. Strong electron-phonon coupling effects are best described in terms of a configurational coordinate, q,[22,36] which is a measure of the lattice distortion near the photoexcited carriers. The fact that the time scale of lattice distortion ($\sim 10^{-13}$ sec) is much longer than that of the electronic transition ($\sim 10^{-16}$ sec) dictates that for such a system the absorption edge is at a higher energy than the emission peak, i.e., a Stokes shift.[22] Since the variation of the excited-state energy with respect to the shifted minimum is quadratic in q, the luminescence line shape becomes a Gaussian with a width which increases with the size of the Stokes shift. The observation of a broad Lorentzian line shape (see Fig. 4) with a small Stokes shift in *cis*-$(CH)_x$ is, therefore, qualitatively different from the typical results obtained from luminescence studies of semiconductors.[22]

The experimental results can be more generally viewed as evidence for the generation of defects, either induced through isomerization or by photogeneration. Related phenomena are well known in tetrahedrally bonded amorphous semiconductors.[36,37] In such materials defects containing a single nonbonding electron give rise to $s=\frac{1}{2}$ states (inside the gap) which tend to quench the photoluminescence. As a result, in such systems higher spin densities correlate with lower quantum efficiency for luminescence.[37] These defect states in glasses can be generated either in the synthesis or by intense laser light[38] at low temperatures. Solitons, the nonlinear excitations of polyacetylene, can be visualized in this context as specific defects in a one-dimensional covalent semiconductor. The photogeneration of soliton-antisoliton pairs in $(CH)_x$ is initiated by the breaking of a π bond, leading to the generation of two nonbonding states which can subsequently diffuse apart. The topology of the bond-alternating one-dimensional conjugated polymer dictates that the presence of such a defect necessarily results in a change in sign of the bond alternation across the defect; i.e., a soliton.

IV. CONCLUSION

The principal conclusion obtained from the photoluminescence and photoconductivity measurements presented in this paper is that the photogenerated carriers in polyacetylene are soliton-antisoliton pairs. In particular, the absence of band edge luminescence in *trans*-$(CH)_x$ and the absence of photoconductivity in *cis*-$(CH)_x$ are of prime importance. The experimental results are summarized in Table I. Luminescence is observed from *cis*-$(CH)_x$, but not from *trans*-$(CH)_x$, whereas photoconductivity is observed in *trans*-$(CH)_x$, but not in *cis*-$(CH)_x$. In *trans*-$(CH)_x$, the degenerate ground state leads to free soliton excitations and photoconductivity. In *cis*-$(CH)_x$ the nondegenerate ground state leads to confinement of the photogenerated carriers, absence of photoconductivity, and to the observed recombination luminescence.

TABLE I. Summary of principal results.

	cis-$(CH)_x$	*trans*-$(CH)_x$
Ground state	Nondegenerate	Degenerate by symmetry
Nonlinear excitation	Confinement	Stable free soliton-antisoliton pair
Band-edge luminescence	Yes	No
Photoconductivity	No	Yes

Previous studies have demonstrated that the novel electronic and magnetic results obtained from undoped and lightly doped polyacetylene can be understood in terms of the soliton model. The existence of the two isomers of polyacetylene has now provided the conceptual and experimental basis for analysis of the photoexcitations in the undoped polymer in terms of photogenerated solitons.

ACKNOWLEDGMENTS

We thank Professor E. Burnstein and Mr. G. W. Ritchie for their generous cooperation in the use of the light scattering equipment needed to obtain the luminescence and Raman spectra presented in this paper. The dye laser was obtained from the Regional Laser Laboratory at the University of Pennsylvania; we thank Dr. G. Holtom and Mr. P. Davis for assistance. It is a pleasure to acknowledge stimulating and important discussions with Professor J. R. Schrieffer, Dr. S. Brazovskii, and Dr. S. Kivelson. The luminescence and Raman studies were supported by the Army Research Office (DAAG29-81-K-0058). Support for the photoconductivity studies and the synthesis, doping, and materials preparation was obtained from DARPA-ONR on a grant monitored by the Office of Naval Research.

---

*Department of Materials Science and Engineering.
†Department of Physics.
‡Department of Chemistry.

[1]W. P. Su, J. R. Schreiffer, and A. J. Heeger, Phys. Rev. Lett. 42, 1698 (1979); Phys. Rev. B 22, 2099 (1980).
[2]M. J. Rice, Phys. Lett. 71A, 152 (1979).
[3]H. Takayama, Y. R. Lin-Liu, and K. Maki, Phys. Rev. B. 21, 2388 (1980).
[4]S. Brazovskii, JETP Lett. 28, 656 (1978) [Zh. Eksp. Teor. Fiz., Pis'ma 28, 606 (1978)]; Sov. Phys. JETP 78, 677 (1980) [Zh. Eksp. Teor. Fiz. 78, 677 (1980)].
[5]B. R. Weinberger, E. Ehrenfreund, A. Pron, A. J. Heeger, and A. G. MacDiarmid, J. Chem. Phys. 72, 4749 (1980).
[6]M. Nechtschein, F. Devreux, R. L. Greene, T. C. Clarke, and G. B. Street, Phys. Rev. Lett. 44, 356 (1980).
[7]K. Holczer, J. P. Boucher, F. Devreux, and M. Nechtschein, Phys. Rev. B 23, 1051 (1981); F. Devreux, K. Holczer, M. Nechtschein, T. C. Clarke, and R. L. Greene, in *Physics in One-Dimension,* edited by J. Bernasconi and T. Schneider, Springer Series on Solid State Sciences (Springer, Berlin, 1980).
[8]C. R. Fincher, Jr., M. Ozaki, A. J. Heeger, and A. G. MacDiarmid, Phys. Rev. B 19, 4140 (1979).
[9]E. Mele and M. J. Rice, Phys. Rev. Lett. 45, 926 (1980).
[10]S. Etemad, A. Pron, A. J. Heeger, A. G. MacDiarmid, E. G. Mele, and M. J. Rice, Phys. Rev. B 23, 5173 (1981).
[11]N. Suzuki, M. Ozaki, S. Etemad, A. J. Heeger, and A. G. MacDiarmid, Phys. Rev. Lett. 45, 1209, 1463(E) (1980).
[12]S. Ikehata, J. Kaufer, T. Woerner, A. Pron, M. A. Druy, A. Sivak, A. J. Heeger, and A.G. MacDiarmid, Phys. Rev. Lett. 45, 1123 (1980).
[13]A. J. Epstein, H. Rommelmann, M. A. Druy, A. J. Heeger, and A. G. MacDiarmid, Solid State Commun. (in press).
[14]M. Peo, H. Förster, K. Menke, J. Hocker, J. A. Gardner, S. Roth, and K. Dransfeld, Solid State Commun. (in press).
[15]W. P. Su and J. R. Schrieffer, Proc. Nat. Acad. Sci. 77, 5626 (1980).
[16]S. Etemad, M. Ozaki, A. J. Heeger, and A. G. MacDiarmid, Chem. Scr. (in press).
[17]S. Brazovskii and N. Kirova, Pis'ma Zh. Eksp. Teor. Fiz. 33, 8 (1981) [JETP Lett. 33 (1981)].
[18]H. Shirakawa and S. Ikeda, Polym. J. 2, 231 (1971); H. Shirakawa, T. Ito, and S. Ikeda, *ibid.* 4, 460 (1973); T. Ito, H. Shirakawa, and S. Ikeda, J. Polym. Sci. Polym. Chem. Ed. 12, 11 (1974); 13, 1943 (1975); H. Shirakawa, T. Ito, and S. Ikeda, Die Macromoleculare Chemie 179, 1565 (1978).
[19]C. R. Fincher, Jr., M. Ozaki, M. Tanaka, D. Peebles, L. Lauchlan, A. J. Heeger, and A. G. MacDiarmid, Phys. Rev. B 20, 1589 (1979), and references therein.
[20]H. Shirakawa and S. Ikeda, Polym. J. 2, 231 (1971); H. Shirakawa, T. Ito, and S. Ikeda, *ibid.* 4, 460 (1973); I. Harada, M. Tasumi, H. Shirakawa, and S. Ikeda, Chem. Lett., 1411 (1978); S. Lefrant, L. S. Lichtmann, H. Temkin, D. B. Fitchen, D. C. Miller, G. E. Whitwell, II, and J. M. Burlitch, Solid State Commun. 29, 191 (1979); H. Kuzmany, Phys. Status Solidi (b) 97, 521 (1980).
[21]L. S. Lichtmann, A. Sarhangi, and D. C. Fitchen, Solid State Commun. 36, 869 (1980).
[22]R. A. Street, Adv. Phys. 25, 397 (1976).
[23]A. Matsui and K. Nakamura, Jpn. J. Phys. Suppl. 6, 1468 (1967).
[24]T. Tani, P. M. Grant, W. D. Gill, G. B. Street, and T. C. Clarke, Solid State Commun. 33, 499 (1980).
[25]M. Ozaki, D. L. Peebles, B. R. Weinberger, A. J. Heeger, and A. G. MacDiarmid, J. Appl. Phys. 51, 4252 (1980), and references therein.
[26]B. R. Weinberger, M. Akhtar, and S. C. Gau, J. Synthetic Met. (in press).
[27]R. C. C. Leite, J. F. Scott, and T. C. Damen, Phys. Rev. Lett. 22, 780 (1969); M. V. Klein and S. P. S. Porto, *ibid.* 782 (1969).
[28]See, for example, R. H. Bube, *Photoconductivity of Solids* (Wiley, New York, 1960), pp. 230, 391.
[29]A. J. Heeger, Comments Solid State Phys. (in press).
[30]D. K. Campbell and A. R. Bishop, Phys. Rev. B (in press).
[31]L. S. Lichtmann and D. B. Fitchen, Bull Am. Phys. Soc. 26, 485 (1981).
[32]See J. D. Dow and D. Redfield, Phys. Rev. B 5, 594 (1972), and references therein.
[33]See, for example, D. M. Pai and R. C. Enck, Phys. Rev. B 11, 5163 (1975).

[34]S. Etemad, T. Mitani, M. Ozaki, T.-C. Chung, A. J. Heeger, and A. G. MacDiarmid, Solid State Commun. (in press).
[35]*Solitons and Condensed Matter Physics,* edited by A. R. Bishop and T. Schneider, Springer Series in Solid-State Sciences (Springer, Berlin, 1978).
[36]"*F*-Centers in Alkali Halides," J. J. Morkham, supplement to *Solid State Physics,* edited by F. Seitz and D. Turnbull (Academic, New York, 1966).
[37]R. A. Street, J. C. Knights, and D. K. Biegelsen, Phys. Rev. B 18, 1880 (1978).
[38]D. K. Biegelsen and R. A. Street, Phys. Rev. Lett. 44, 803 (1980).